AGU PUBLICATIONS

JGR

Journal of Geophysical Research: Biogeosciences

RESEARCH ARTICLE
10.1002/2016JG003608

Key Points:
- Interannual variability in atmospheric river landfalls influences vegetation production and fire in dryland ecosystems in the southwest U.S.
- Influences were observed up to 1300 km inland and were most pronounced for those making landfall between 27.5° and 32.5° latitude
- Understanding how atmospheric rivers influence ecosystems provides opportunities to anticipate responses to climate and climate change

Correspondence to:
C. M. Albano,
christine.albano@dri.edu

Citation:
Albano, C. M., M. D. Dettinger, and C. E. Soulard (2017), Influence of atmospheric rivers on vegetation productivity and fire patterns in the southwestern U.S., *J. Geophys. Res. Biogeosci.*, *122*, 308–323, doi:10.1002/2016JG003608.

Received 1 SEP 2016
Accepted 19 JAN 2017
Accepted article online 26 JAN 2017
Published online 8 FEB 2017

Influence of atmospheric rivers on vegetation productivity and fire patterns in the southwestern U.S.

Christine M. Albano[1], Michael D. Dettinger[2], and Christopher E. Soulard[3]

[1]Desert Research Institute, University of Nevada, Reno, Reno, Nevada, USA, [2]National Research Program, U.S. Geological Survey, Carson City, Nevada, USA, [3]Western Geographic Science Center, U.S. Geological Survey, Menlo Park, California, USA

Abstract In the southwestern U.S., the meteorological phenomenon known as atmospheric rivers (ARs) has gained increasing attention due to its strong connections to floods, snowpacks, and water supplies in the West Coast states. Relatively less is known about the ecological implications of ARs, particularly in the interior Southwest, where AR storms are less common. To address this gap, we compared a chronology of AR landfalls on the west coast between 1989 and 2011 and between 25°N and 42.5°N to annual metrics of the normalized difference vegetation index (NDVI; an indicator of vegetation productivity) and daily resolution precipitation data to assess influences of AR-fed winter precipitation on vegetation productivity across the southwestern U.S. We mapped correlations between winter AR precipitation during landfalling ARs and (1) annual maximum NDVI and (2) area burned by large wildfires summarized by ecoregion during the same year as the landfalls and during the following year. Interannual variations of AR precipitation strongly influenced both NDVI and area burned by wildfire in some dryland ecoregions. The influence of ARs on dryland vegetation varied significantly depending on the latitude of landfall, with those ARs making landfall below 35°N latitude more strongly influencing these systems, and with effects observed as far as 1300 km from the landfall location. As climatologists' understanding of the synoptic patterns associated with the occurrence of ARs continues to evolve, an increased understanding of how AR landfalls, in aggregate, influence vegetation productivity and associated wildfire activity in dryland ecosystems may provide opportunities to better predict ecological responses to climate and climate change.

1. Introduction

Atmospheric rivers (ARs) are a major mechanism for water vapor transport from the tropics to midlatitudes that strongly influence precipitation in western North America and elsewhere in the world [*Dettinger and Ingram*, 2013]. In the U.S., this meteorological phenomenon has gained increasing attention in the atmospheric and hydrologic sciences because of its implications for water resources and flood hazards. For example, 30–60% of water supplies in the Sierra Nevada are associated with precipitation coming from ARs [*Guan et al.*, 2010; *Dettinger et al.*, 2011], and these events play a disproportionate role in ending droughts along the west coast [*Dettinger*, 2013]. In addition, ARs have generated 92% of the largest ever storms in the Coastal Ranges and Sierra Nevada of California [*Ralph and Dettinger*, 2012] and are responsible for about 80% of the most extreme floods in the Pacific Coast states [*Ralph et al.*, 2006; *Neiman et al.*, 2008; *Florsheim and Dettinger*, 2015]. Despite their clear influence on hydroclimatic variability in the coastal to interior Southwest regions [*Neiman et al.*, 2013; *Rutz et al.*, 2014; *Alexander et al.*, 2015], little attention has been paid thus far to the influence of these meteorological features on terrestrial ecosystems. In this study, our objective is to assess the extent to which the occurrence of ARs, in aggregate, explains variations in vegetation productivity and fire patterns across the southwestern U.S. Understanding of the role of ARs in the functioning of terrestrial ecosystems, together with rapidly evolving improvements to predictions and projections of these events [e.g., *Dettinger*, 2011; *Guan et al.*, 2012; *Warner et al.*, 2014; *Hagos et al.*, 2016], has the potential to allow scientists and managers to better anticipate and manage ecological responses to hydroclimatic variability and change.

ARs have the potential to affect terrestrial ecosystems both acutely (i.e., in individual AR storms) and in aggregate (i.e., cumulative impacts of multiple storms). Despite the fact that ARs are fleeting events, lasting only a day or two above a given locale, the more extreme episodes can result in step changes in ecosystems by causing mass erosion and slope movements and by windthrow and avalanche impacts on vegetation. Although there has not yet been a comprehensive study linking AR events to geomorphic or vegetation

changes in terrestrial systems, these types of impacts are well documented in river systems [e.g., *Ralph et al*., 2006; *Florsheim and Dettinger*, 2015]. Beyond these impacts, aggregate effects of ARs may include the enhancement of vegetation productivity, soil moisture storage [*Ralph et al*., 2013], and fuel loading, particularly in dryland (i.e., arid to semiarid grassland and shrubland) ecosystems, where water availability limits plant growth.

AR influences on precipitation vary significantly across the southwestern U.S. Precipitation from ARs varies along two major geographic gradients—from north to south and from coastal to inland. Generally speaking, ARs decrease in frequency and duration along the U.S. west coast from north to south [*Rutz et al*., 2014] but reach their strongest intensities in Northern California, resulting in greatest average AR-precipitation fractions (proportion of total precipitation at a given location that occurs on AR landfall dates) in northern and central California, declining somewhat to the north and more so to the south [*Dettinger et al*., 2011; Rutz *et al*., 2014]. Topography controls the coastal to inland gradient, with most AR precipitation taking the form of orographic precipitation, occurring mostly to the west of major topographic barriers such as the Sierra Nevada and Cascade ranges [*Rutz et al*., 2014]. Given these gradients, the interior Southwest receives less total AR precipitation, on average [*Rutz et al*., 2014]. However, in some years when large or numerous ARs make landfall in Southern California or Baja California, the contribution of ARs to winter precipitation in this region can be significant, because gaps in the topographic barriers exist, allowing penetration further inland [*Rutz and Steenburgh*, 2012; *Neiman et al*., 2013; *Rutz et al*., 2014]. Moreover, the effects of these inland penetrations can be strongly influenced by the angle of orientation at which ARs make landfall [*Ralph et al*., 2003; *Hughes et al*., 2014]. This results in large interannual variations of both AR and total precipitation in the interior Southwest, which can, in turn, have significant effects on vegetation biomass production in dryland ecosystems [*Notaro et al*., 2010].

Scientists' understanding of linkages between AR activity along the west coast and broader-scale ocean-atmosphere patterns is at an early stage (i.e., the few papers on this topic have been published within the last 5 years) but is rapidly evolving. At intraseasonal time scales, the Madden-Julian Oscillation has been found to modulate AR activity over the Northeast Pacific and West Coast [*Guan et al*., 2012; *Jones and Carvalho*, 2014], which may have important implications for short-term (weeks to months) weather, storm, and water supply forecasting. Linkages between ARs and interannual climate modes remain uncertain. For example, *Dettinger et al*. [2011] identified positive correlations between the fraction of total precipitation that derives from landfalling Pineapple Express storms (a subset of ARs that follow a linear, southwesterly trajectory from the East Pacific tropics or subtropics to U.S. West Coast, see *Dettinger et al*., 2011) and sea-surface temperature indices of the El Niño-Southern Oscillation (ENSO) and the Pacific Decadal Oscillation (PDO). However, using different metrics of AR activity, other studies have found no link between AR occurrences and ENSO [e.g., *Rivera et al*., 2014]. At decadal time scales, the positive phase of the PDO and negative phase of the North Pacific Gyre Oscillation appear to be associated with more numerous ARs over the northeast Pacific [*Liu et al*., 2015]. If such linkages can be isolated and used for intraseasonal to interannual forecasting of AR statistics, that predictability ultimately could have important implications for flood and water resources management as well as for land and wildfire management (as indicated by the present study).

Patterns of wildfire in western ecosystems are strongly influenced by climate on multiple time scales. Regional-scale synchronies in fire activity in the Southwest have been observed in conjunction with ENSO [*Swetnam and Betancourt*, 1997], and more recently with interacting phases of the Pacific Decadal Oscillation, ENSO, and the Atlantic Multidecadal Oscillation [*Kitzberger et al*., 2007]. On shorter time scales, near-term antecedent (i.e., 1–3 years preceding; *Westerling et al*., 2003; *Crimmins and Comrie*, 2004; *Littell et al*., 2009) atmospheric conditions are also strongly associated with fire activity. The primary mechanism by which near- and long-term antecedent conditions influence fire patterns is by modulating fuels accumulation (i.e., aboveground biomass production) and fuel moisture that, when coupled with short-term or concurrent meteorological conditions, strongly influence fire occurrence and severity [*Abatzoglou and Kolden*, 2013]. Uncovering these patterns has provided important and useful information for predicting potential fire activity [*Owen et al*., 2012].

To the extent that AR landfalls have impacted precipitation, vegetation, and wildfire risk across the Southwest, the variability of those AR landfalls must be an important facet of the climatic conditions that southwestern vegetation and landscapes have accommodated and adapted to during the late Holocene.

Understanding relations between ARs and landscapes may improve our understanding of the conditions—and especially the kinds of extreme climatic events—that southwestern landscapes need to survive and flourish in the long term. Efforts to preserve, restore, or adapt western landscapes to future climate changes are likely to benefit from studies, like this one, that catalog historical relations between AR landfalls and landscape variability, so that future relations might be more predictable.

To the extent that AR statistics may eventually be predictable on time scales from seasons and years [*Mundhenk et al*., 2016; *Ralph et al*., 2016] to those of long-term climate changes [*Dettinger*, 2011], any linkages that can be identified between ARs and vegetation biomass production, and between ARs and antecedent fuel conditions, may allow insights and predictions of future ecosystem and wildfire conditions. Annual AR frequencies, landfall latitudes, and amplitudes are reasonably well represented in weather forecasting and general circulation models [*Wick et al*., 2013; *Payne and Magnusdottir*, 2015], suggesting that skillful forecasts and projections of such ARs and responses may become possible in the future. This study assesses historical relations between landfalling ARs and interannual variations in vegetation biomass production and associated fuels accumulation in the Southwest. The relations identified are stratified in terms of AR landfall latitude, the influence of topographic barriers, and across ecosystem types.

2. Data and Methods

Our study area includes four southwestern states: California, Nevada, Utah, and Arizona (Figure 1). To quantify AR precipitation and effects, we used a daily chronology of ARs making landfall between 27.5°N and 42.5°N latitudes in 2.5° increments (generated by J. Rutz, NWS Salt Lake City). The AR chronology was developed by the procedure used in *Rutz and Steenburgh* [2012] using NCEP-NCAR Reanalysis fields [*Kalnay et al*., 1996], which are consistent with the reanalysis product used in *Rutz and Steenburgh* [2012] in terms of AR detection during the time period we analyzed [*Lavers et al*., 2012; *Brands et al*., 2016]. The chronology was used to identify the dates and latitudes of AR landfalls during water years 1989–2011. We calculated the vapor transport direction at landfall relative to due east for each AR at a given landfall latitude as the arcsine of the ratio of eastward to total integrated water vapor transport (IVT). We then categorized each AR's vapor transport direction into the following classes: South < -67.5, Southeast -67.5 – 22.5°, East -22.5 – 22.5° Northeast 22.5–67.5°, North > 67.5 (see Figure 2). Next, we used 4 km daily precipitation data [*Abatzoglou*, 2013] to calculate the sum of precipitation at each 4 km pixel that occurred on winter (October–April) dates with AR landfalls at each of the eight coastal latitudes considered here in each water year and to calculate total precipitation for each water year. We included this 7 month winter season, because this captures the time period when most AR landfalls and AR precipitation occur within the part of the west coast studied here [*Neiman et al*., 2008; *Rutz et al*., 2014]. We also focus on winter precipitation because it strongly influences peak vegetation productivity in most of our study area, where winter rains and eventual snowmelt contribute most to deep soil moisture conditions [*Notaro et al*., 2010]. To characterize the extent to which winter ARs influence interannual variation in precipitation across our study region, we calculated the Spearman rank correlation coefficients (r) between winter AR precipitation associated with each landfall latitude and total winter precipitation across the study period for each pixel. We report all p-values based on two-sided probabilities.

ARs are moving features that (also) impact latitudes beyond those of their initial landfall. They tend to sweep southward along the west coast, from the location of their initial landfall, until they deteriorate to the point of no longer constituting an AR. The results we report related to landfall latitudes are meant to characterize how ARs influence ecosystems of the Southwest based on their geographic tendencies, but because of this movement, these latitude-specific results are not independent of one another. To characterize among-latitude dependencies, we quantified the cooccurrence of ARs across latitudes based on the fraction of AR days on which ARs were reported to be making landfall at more than one latitude.

We used the annual maximum normalized difference vegetation index (NDVI) from 1989 to 2011 as a proxy for annual aboveground vegetation biomass production [*Pettorelli et al*., 2005], based on advanced very high resolution radiometer (1 km resolution) data available from the USGS Earth Resources Observation and Science Center (http://phenology.cr.usgs.gov). This NDVI product benefits from close attention to compositing and smoothing to eliminate noise relative to alternative unprocessed data sets [*Swets et al*., 1999] and also provides higher spatial resolution than global alternatives [*Eidenshink*, 2006]. We calculated Spearman's rank

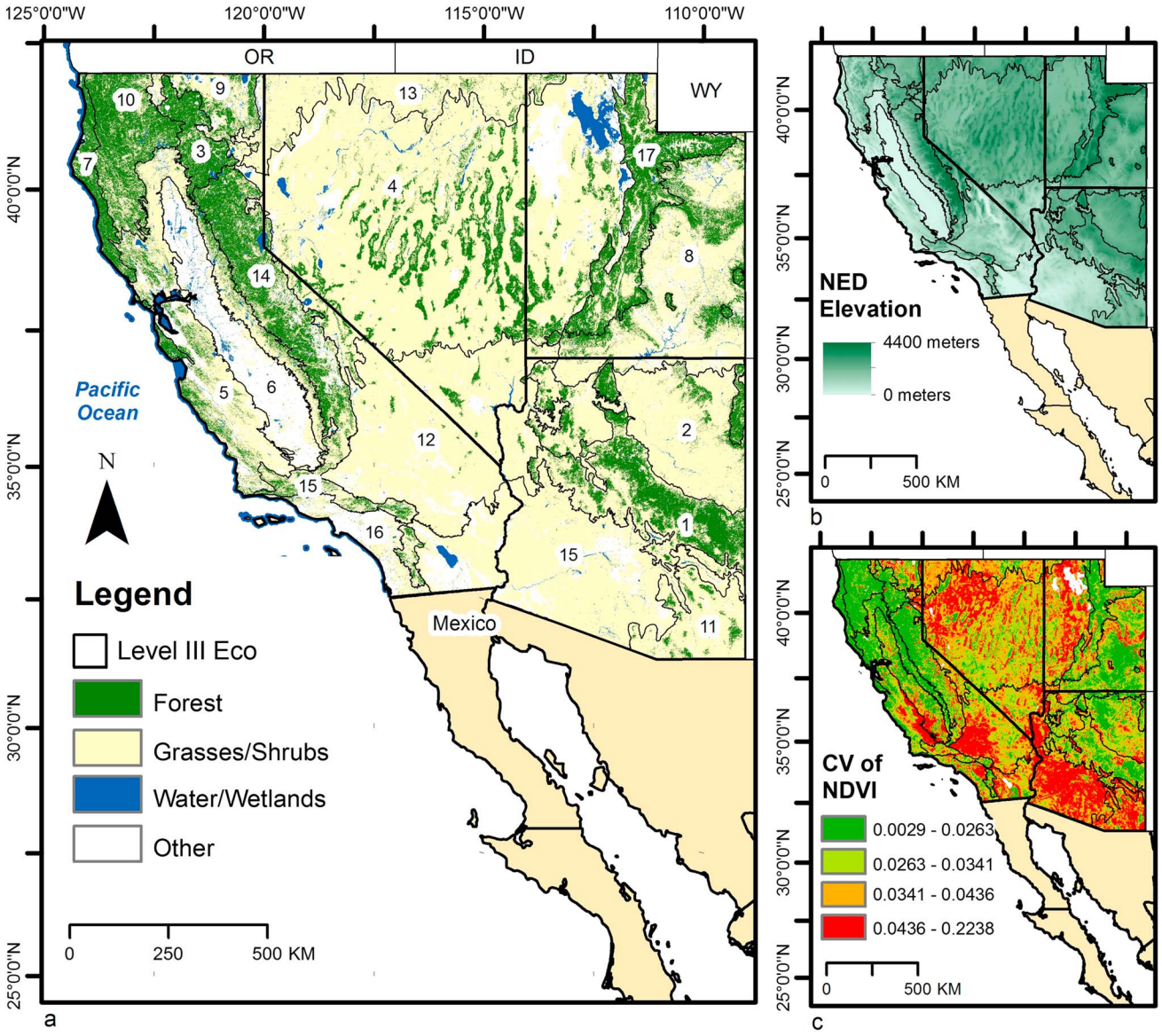

Figure 1. Geographic distributions of (a) ecosystem types and Level III ecoregions [*Environmental Protection Agency*, 2013; see Table 2 for ecoregion names], (b) National Elevation Database (NED) elevation, and (c) coefficient of variation (CV) of annual maximum NDVI across the study region.

correlations between winter AR precipitation at each landfall latitude and annual maximum NDVI at each 1 km pixel. We summarized the AR-vegetation relationship by identifying the maximum correlation coefficient (r) for each pixel and the AR-landfall latitude that yielded that correlation. We repeated this analysis using the Enhanced Vegetation Index (EVI) data set, which is more sensitive to variation in high-biomass regions [*Ji and Peters*, 2007] and, as expected given tendencies for EVI and NDVI to be correlated, found these results to be consistent with those from the NDVI analysis presented here.

To characterize wildfire histories in relation to ARs, we summarized fire histories for Level IV ecoregions [*Environmental Protection Agency*, 2013] using georeferenced fire area for 1989–2012 from the Monitoring Trends in Burn Severity (MTBS) Project [*MTBS*, 2016a]. The Level IV ecoregions are broad, often discontiguous areas delineated based on ecological similarities within a given Level III ecoregion (Figure 1). The 17 Level III and 268 Level IV ecoregions average approximately 70,000 and 5000 km^2 in size, respectively. We sorted burned area perimeters detected from postfire imagery annually, excluding prescribed fires [*MTBS*, 2016a]. Within these perimeters, we selected pixels with burn severity classes 1–6 [*MTBS*, 2016b] to develop summaries of annual area burned by wildfire for each ecoregion. We calculated a spatial average of annual AR

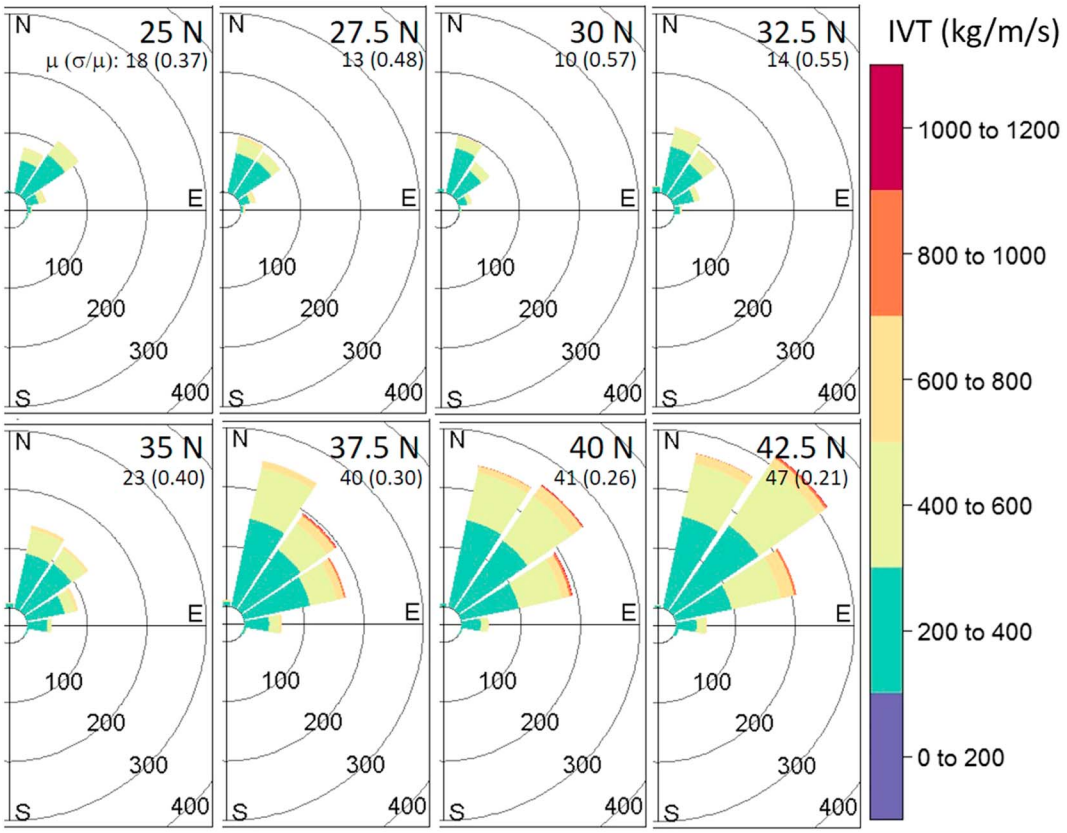

Figure 2. Overall frequencies of winter ARs by latitude (25–42.5 N) from 1989–2011, vapor-transport direction at landfall, and intensity (as indicated by integrated water vapor transport; IVT). For each latitude, the mean annual winter AR frequency (μ) and the coefficient of variation (σ/μ) of the annual frequency are included.

precipitation within each ecoregion, and Spearman's rank correlated this with annual area burned for the same year (i.e., during the latter half of the winter season and the 8 months following), and with a 1 year lag (i.e., 9–18 months later). For example, correlations between AR precipitation from October 1995 to April 1996 and area burned by wildfire during the January 1996 to December 1996 time period are identified as "same year," and correlations between AR precipitation from the same time period with area burned by wildfire during the January 1997 to December 1997 time period are identified as "1 year lag." This lag was included because fire activity frequently exhibits a 1 year lagged response in many western ecosystems [*Westerling et al*., 2003; *Littell et al*., 2009].

We evaluated temporal autocorrelations by calculating Spearman's rank correlation coefficients for each variable (annual AR precipitation by latitude, maximum NDVI, and annual area burned by ecoregion) based on 1 and 2 year lags. We also conducted Mann-Kendall slope tests for temporal trend for each of these variables. Autocorrelation and trends were (1) not significant for AR precipitation, (2) significant for annual maximum NDVI in some forested regions, where relationships identified in our analysis were generally weak, and (3) autocorrelation was significant for 1 year lags of annual area burned in semiarid regions, but not for 2 year lags, nor were long-term trends significant in these regions. Because adjustments for effective sample size are only substantial if both predictor and response variables are temporally autocorrelated, there was no need to adjust effective sample sizes [*Dawdy and Matalas*, 1964].

3. Results

3.1. Winter AR Occurrence and Distribution

The latitudinal distribution of annual frequencies of landfalling winter ARs varied along the west coast, with frequencies generally increasing from south to north and with ARs occurring at 37.5°N and above having

Table 1. Cooccurrence of Winter (October-April) Atmospheric River Landfall Across Latitudes, 1989–2011[a]

	Landfall Latitude (Degrees North)	B							
		42.5|	40|	37.5|	35|	32.5|	30|	27.5|	25|
A	|42.5	**1.00**	**0.72**	**0.52**	0.21	0.08	0.03	0.02	0.02
	|40	**0.84**	**1.00**	**0.73**	0.32	0.12	0.05	0.04	0.02
	|37.5	**0.63**	**0.78**	**1.00**	0.43	0.18	0.08	0.06	0.03
	|35	0.44	**0.57**	**0.74**	**1.00**	0.46	0.20	0.14	0.05
	|32.5	0.26	0.33	0.46	**0.69**	**1.00**	0.48	0.33	0.10
	|30	0.14	0.18	0.28	0.43	**0.69**	**1.00**	**0.67**	0.25
	|27.5	0.10	0.14	0.19	0.26	0.42	**0.60**	**1.00**	0.45
	|25	0.06	0.07	0.08	0.08	0.12	0.20	0.42	**1.00**

[a]Table values represent the proportion of dates an AR makes landfall at latitude B, given landfall occurrence at latitude A (Pr (B|A)). Proportions greater than 0.5 are highlighted in bold.

generally higher intensities, as indicated by IVT (Figure 2). The coefficients of variation of annual AR frequencies are largest for ARs making landfall at 27.5°N–32.5°N (Figure 2), indicating that interannual variability in AR frequencies at southern latitudes is high relative to their mean frequencies. These patterns are consistent with overall low mean contributions of ARs to precipitation in the interior Southwest and high interannual variability (see *Rutz et al.* [2014] for a thorough review of the climatological characteristics of ARs in this region). Across all latitudes, most landfalling winter ARs were oriented toward the northeast, with fewer occurring with northward or eastward orientation and almost none occurring with southeastward or southward orientations (Figure 2). Our analysis of AR landfall cooccurrence across latitudes indicates that ARs occurring at latitudes north of 35°N frequently make landfall across three or more latitudes in a single day, while ARs arriving between 27.5°N and 32.5°N latitude more typically cooccur across two latitudes rather than three, and overall cooccur less frequently than those at higher latitudes (Table 1). ARs making landfall at 25°N had the least cooccurrence with ARs at other latitudes in our study area. Thus, northern AR landfalls traverse and impact longer along-coast distances in a single day than ARs arriving farther south because of different coastal orientations. South of about 35°N, where the coastline is oriented NW-SE (as opposed to more N-S orientation further North), an AR with equal speed and orientation would need to travel along a longer length of coastline to traverse the same latitude band than an AR making landfall further to the north. Because an AR tends to make its landfall on multiple latitudes on most days (Table 1), there is an ambiguity regarding the attributions of AR landfalls at various latitudes to the various southwestern conditions in the results that follow; however, because most of this study addresses seasonal scale totals and correlations, the ambiguity is not of great concern here.

3.2. AR Precipitation

Correlations between winter AR precipitation and total winter precipitation vary geographically with landfall latitude (Figure 3) and in relation to topographic barriers. Correlations were generally greater than $r = 0.7$ ($p < 0.001$) across much of AZ, southern CA, as well as across the Central Basin and Range in Nevada (Figures 1 and 3) for ARs making landfall between 27.5°N and 32.5°N latitudes. At more northern latitudes (35°N–42.5°N), correlations were low to the east of the Sierra Nevada Mountains, in the Central Basin and Range, but correlations were high as far inland as northern UT to the north of the Sierras. Notably these figures differ from those reported by *Rutz et al.* [2014], despite the use of the same AR detection methods, because the *Rutz et al.* [2014] maps of AR-precipitation fractions corresponded to mean AR contributions rather than correlations between AR precipitation and total winter precipitation variations and also because *Rutz et al.* [2014] analyzed for ARs overhead at each inland locale, whereas Figure 3 reflects the relations between where ARs make landfall and inland precipitation. Because of this latter strategy, Figure 3 is able to discretize AR contributions to precipitation variability as a function (in separate panels) of landfall location. This discretization allows us to recognize contributions to precipitation from distant AR landfalls (e.g., the unexpectedly large contributions of AR landfalls at 35°N to precipitation along the northern (42.5°N) extremes of the study area shown in Figure 3).

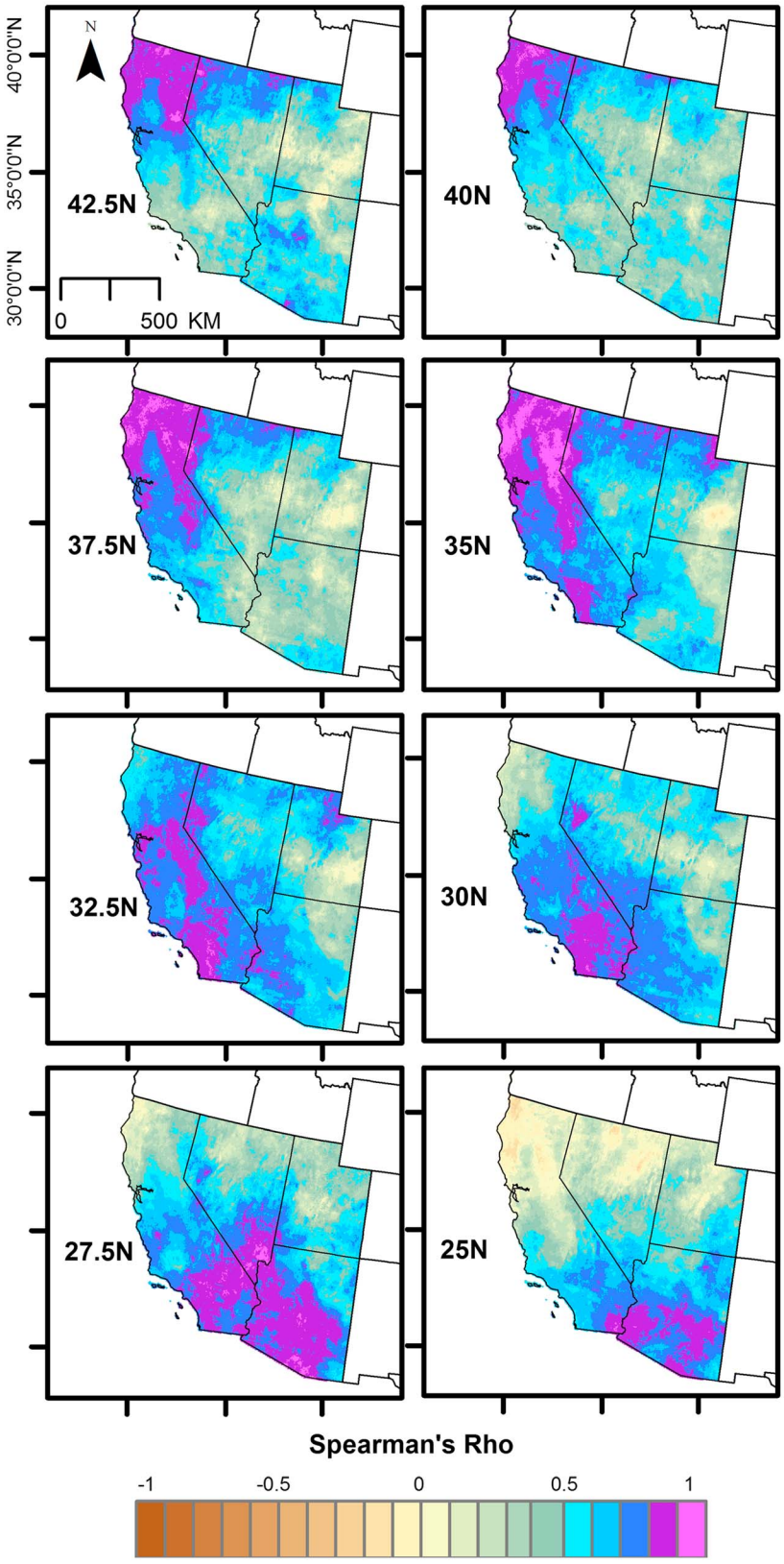

Figure 3. Spearman's rank correlation coefficient (*r*) between total annual winter precipitation and total winter precipitation occurring on AR landfall dates, by latitude of landfall, 1989–2011. *r*-values > 0.5 (significant at $p = 0.02$) are highlighted in blue to purple tones.

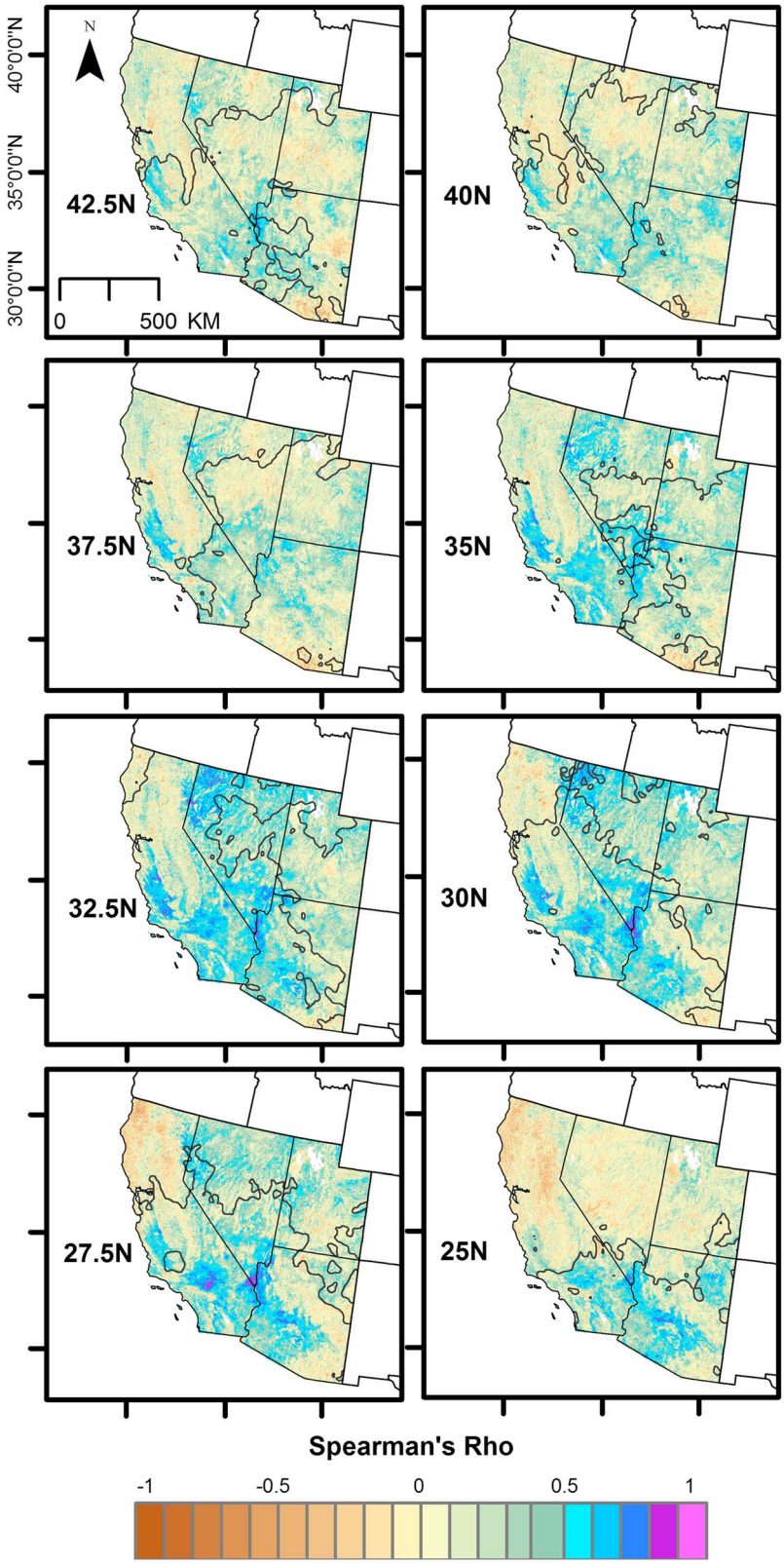

Figure 4. Spearman's rank correlations (*r*) between annual winter atmospheric river precipitation and annual maximum NDVI during the subsequent growing season by latitude of landfall, 1989–2011. *r*-values > 0.5 (significant at $p = 0.02$) are highlighted in blue to purple tones. Contours delineate areas where $r > 0.6$ between annual winter AR and total winter precipitation (see Figure 3).

Table 2. Spatial Summaries of Results Within EPA Level III Ecoregions and Dominant Land Cover Types (See Figure 1)

	Proportion of Land Cover Type Within Ecoregion		Mean (Standard Deviation) Maximum Correlation Between Annual Winter AR Precipitation and Maximum NDVI Across Landfall Latitudes		Mean AR Landfall Latitude of Maximum Correlation Between Annual Winter AR	Area-Weighted Mean Maximum Correlation Between Annual Winter AR Precipitation and Area Burned by Wildfire Across Landfall Latitudes	
Level III Ecoregion	Forest/ Woodland	Grassland/ Shrubland	Forest/ Woodland	Grassland/ Shrubland	Precipitation and Maximum NDVI	Same year	1 year lag
1. Arizona/New Mexico Mountains	0.54	0.45	0.32 (0.14)	0.37 (0.17)	35.3	−0.11	0.35
2. Arizona/New Mexico Plateau	0.09	0.87	0.37 (0.14)	0.40 (0.15)	31.6	0.11	0.22
3. Cascades	0.78	0.18	0.21 (0.13)	0.23 (0.14)	32.8	0.12	0.04
4. Central Basin and Range	0.12	0.74	0.35 (0.14)	0.46 (0.15)*	31.5	0.18	0.48*
5. Central California Foothills/Coastal Mountains	0.17	0.65	0.28 (0.17)	0.43 (0.20)	33.4	0.18	0.19
6. Central California Valley	0.00	0.16	0.24 (0.16)	0.41 (0.22)*	32.2	0.34	0.24
7. Coast Range	0.74	0.15	0.21 (0.14)	0.21 (0.16)	37.0	0.24	0.07
8. Colorado Plateaus	0.24	0.62	0.43 (0.13)*	0.42 (0.14)*	34.2	0.03	0.33
9. Eastern Cascades Slopes and Foothills	0.42	0.43	0.30 (0.15)	0.39 (0.17)	30.1	0.12	0.24
10. Klamath Mountains/California High North Coast Range	0.65	0.27	0.27 (0.14)	0.28 (0.15)	36.4	0.04	0.07
11. Madrean Archipelago	0.08	0.88	0.26 (0.16)	0.22 (0.16)	29.7	0.18	0.11
12. Mojave Basin and Range	0.02	0.88	0.25 (0.2)	0.56 (0.15)**	31.6	0.29	0.55**
13. Northern Basin and Range	0.03	0.89	0.44 (0.14)*	0.54 (0.14)**	30.9	0.18	0.46*
14. Sierra Nevada	0.54	0.37	0.23 (0.14)	0.31 (0.16)	32.3	0.00	0.20
15. Sonoran Basin and Range	0.00	0.80	0.38 (0.13)	0.52 (0.15)**	30.5	0.40	0.26
16. Southern California Mountains	0.28	0.66	0.23 (0.15)	0.36 (0.18)	33.9	0.00	0.31
17. Southern California/Northern Baja Coast	0.02	0.47	0.40 (0.15)	0.53 (0.14)**	32.8	0.38	0.21
18. Wasatch and Uinta Mountains	0.63	0.32	0.35 (0.14)	0.38 (0.14)	33.4	0.04	0.25

*Statistical significance at $p = 0.05$.
**Statistical significance at $p = 0.01$.

3.3. Vegetation Biomass Production

Correlations between winter AR precipitation and annual maximum NDVI also varied with latitude of landfall, in broad geographic patterns that reflect differences between forested and dryland ecosystems as well as the effects of topographic barriers (Figure 4 and Table 2). Starting from the south, AR precipitation associated with southern (25°N–35°N) landfalling ARs are—as might be expected—most positively correlated with maximum NDVI in the southern parts of the study area, the Mojave and Sonoran Basin and Range ecoregions. However, ARs making landfall between 30°N and 35°N latitudes are also significantly correlated with maximum NDVI in the Northern Basin and Range ecoregion in northwestern NV, far to the north of landfalls and on the leeward side of the great Sierra Nevada topographic barrier. Correlations between maximum NDVI and AR precipitation associated with 37.5°N latitude and farther north become increasingly weak. Maximum correlations among landfall latitudes between winter AR precipitation and NDVI ranged widely depending on ecoregion and vegetation types, with Level IV ecoregional averages ranging between 0.1 ($p = 0.65$) and 0.70 ($p < .001$; Figure 5b) and with Level III ecoregional averages ranging between 0.21 ($p = 0.34$) and 0.56 ($p = 0.01$; Table 2), depending on the vegetation type. ARs making landfall between 27.5°N and 32.5°N had the most widespread effects on maximum NDVI across the study region (Figure 5c).

Viewed from the perspectives of broader, Level III ecoregions and dominant land cover types, maximum NDVI in ecoregions that are dominantly forested (e.g., in northern CA and in parts of AZ and UT; Figure 1) was generally not as sensitive to winter AR precipitation as that in other ecoregions (Table 2). Maximum NDVI in the most arid ecoregions in the study area, including the Mojave, Sonoran, Central, and Northern Basin and Range ecoregions, Southern California, and Central California Foothills and Mountains ecoregions (where vegetation ranges from semidesert scrub and grasslands to Pine-Oak woodlands) were more responsive to AR precipitation, and those regions almost universally respond most to AR landfalls far to the south, as evidenced by the maximum correlation coefficient across latitudes (Figures 5b and 5c and Table 2).

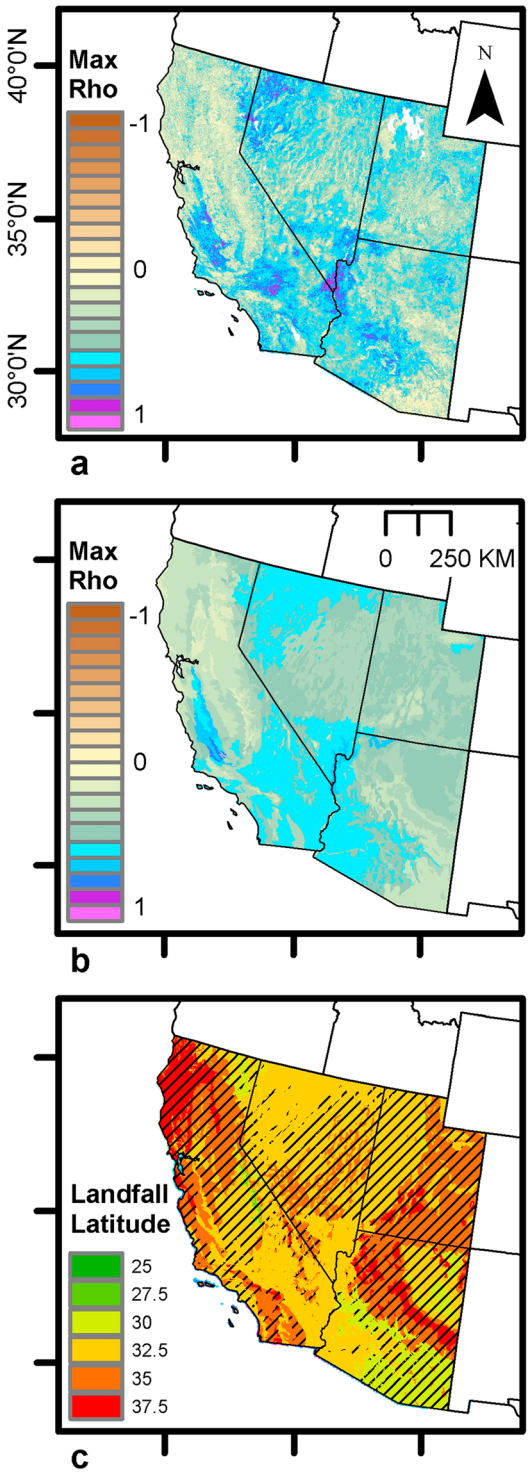

Figure 5. Maximum Spearman's rank correlation (*r*) between annual winter atmospheric river precipitation and annual maximum NDVI (a) across all latitudes of landfall and (b) across all latitudes of landfall, averaged by EPA Level IV Ecoregion. *r*-values > 0.5 (significant at $p = 0.02$) are highlighted in blue to purple tones. (c) Average landfall latitude of the maximum Spearman's rank correlation between winter atmospheric river precipitation and maximum NDVI by EPA Level IV Ecoregion. Hash-marked areas indicate areas where maximum *r* between winter atmospheric river precipitation and maximum NDVI is < 0.5 (significant at $p = 0.02$).

3.4. Wildfires

The highest correlations (up to $r = 0.74$, $p < 0.01$) between AR precipitation and area burned by wildfire generally occur in the more arid parts of our study area (Figures 6 and 7), where AR-NDVI correlations are also highest. Conversely, correlations between winter AR precipitation and area burned are generally low in forested regions. Across the study extent, correlation coefficients were generally higher and more positive for the 1 year lag (Figure 7), than for the same year, which exhibited a larger range of positive to negative correlation values (Figure 6). Significant, positive correlations between winter AR precipitation and area burned by wildfire in the same year occurred in a few Level IV ecoregions in Southern California (up to $r = 0.57$, $p < 0.01$), Central California Foothills and Mountains (up to $r = 0.65$, $p = 0.01$), and Sonoran Desert (up to $r = 0.53$, $p < 0.01$; Figure 6), but overall mean correlations at the Level III ecoregion scale were not significant (Table 2). In contrast, AR precipitation and area burned by wildfire the following year (1 year lag; Figure 7) exhibit relatively widespread positive, significant correlations where AR precipitation and maximum NDVI were also significantly correlated in the western Mojave, Northern, and Central Basin and Range ecoregions (Figures 4 and 7 and Table 2). In these regions, grasses and forbs are the primary fuels for wildfire. AR precipitation contributes to soil moisture that promotes the rapid growth of these plants, but this moisture itself may initially (i.e., in the same year) inhibit the spread of wildfire until drier conditions prevail and the fuels dry, yielding the lagging correlation response [*Westerling et al.*, 2003].

4. Discussion

These results indicate that interannual variations in AR precipitation are associated with variations in vegetation productivity in dryland ecosystems across the study area, particularly in the Mojave, Central, Northern, and

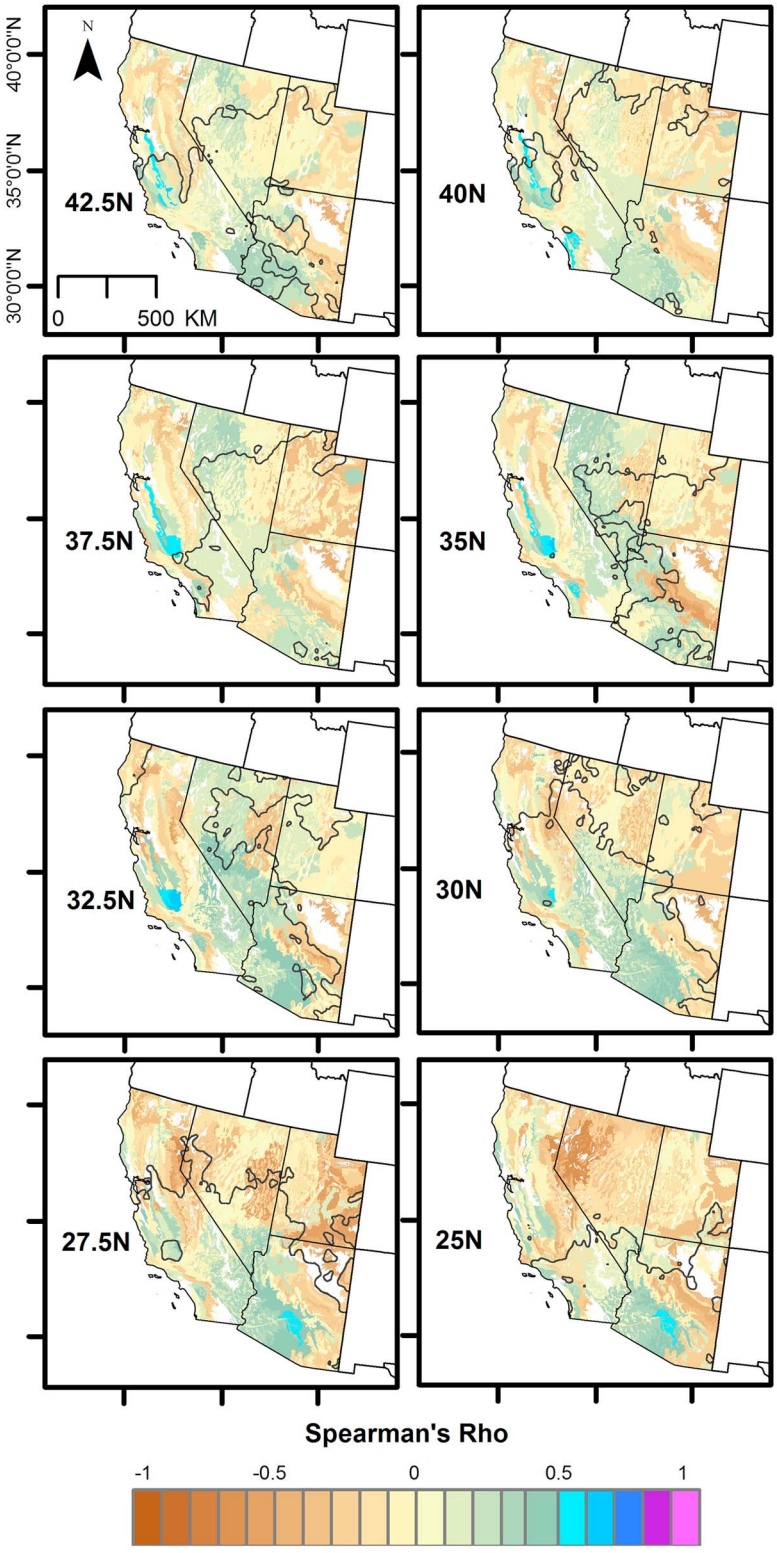

Figure 6. Spearman's rank correlations (*r*) between winter atmospheric river (AR) precipitation by latitude and water year, averaged across EPA level IV ecoregions and area burned by wildfire during the latter half of the winter season and the 8 months following (same year) for the 1989–2012 study period. For example, AR precipitation from October 1995 to April 1996 is correlated with area burned by wildfire during the January 1996 to December 1996 time period. *r*-values > 0.5 (significant at $p = 0.02$) are highlighted in blue to purple tones. Contours delineate areas where $r > 0.6$ between annual winter AR and total winter precipitation (see Figure 3).

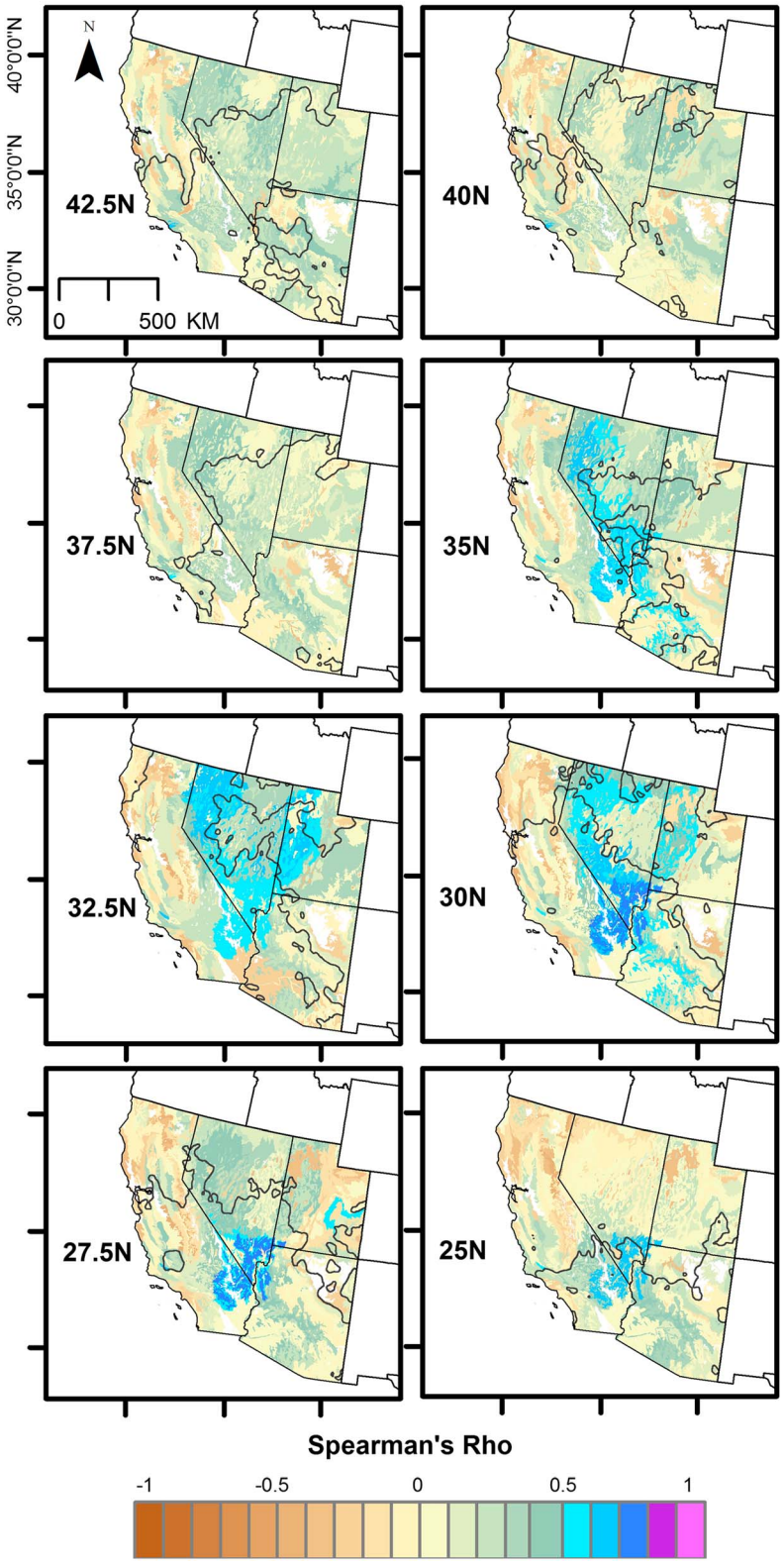

Figure 7. Spearman's rank correlations (*r*) between winter atmospheric river (AR) precipitation by latitude and water year, averaged across EPA level IV ecoregions, and area burned by wildfire 9–18 months later (1 year lag) for the 1989–2012 study period. For example, AR precipitation from October 1995 to April 1996 is correlated with area burned by wildfire during the January 1997 to December 1997 time period. *r*-values > 0.5 (significant at $p = 0.02$) are highlighted in blue to purple tones. Contours delineate areas where $r > 0.6$ between annual winter AR and total winter precipitation (see Figure 3).

Sonoran Basin and Range provinces and in the lowlands ecoregions of Central and Southern California. This AR footprint is cogent and is primarily driven by the occurrence of relatively infrequent AR landfalls between 27.5 N and 32.5 N latitudes (Figure 4). The influence of ARs on vegetation productivity and associated fuels accumulation (implied by the NVDI correlations) is enough so that these events alone correlate statistically significantly with temporal variation of fire activity in the Mojave, Central, and Northern Basin and Range ecoregions (Figures 6 and 7).

4.1. Winter AR Influences on Vegetation Biomass Production

The strength of correlations between winter AR precipitation and maximum NDVI varied substantially over the study region and covaried with several factors. First, correlations between AR precipitation and NDVI are strongest in the most arid parts of the study region, which generally receive less than 10 cm average annual precipitation (*Daly et al*., 2008; http://prism.oregonstate.edu/). Water availability strongly controls aboveground vegetation production in dryland systems, whereas photoperiod and temperature are the primary controls in forested systems [*Knapp and Smith*, 2001] where interannual variability in NDVI tends to be low [*Reed et al*., 1994].

Although we do not present the results of these analyses here, we also explored other facets of interannual variability in ARs and found similar but weaker correlation patterns. These other facets included the following: (1) correlations between the number of AR landfall days (rather than precipitation amounts on those days) and maximum NDVI and (2) correlations between the precipitation amounts from a subset of ARs with landfall IVT values greater than 500 kg/m/s and maximum NDVI. The weaker correlations in these two instances suggest that the cumulative amount of precipitation is more important than the frequency (in the first case) or intensity (in the second case) of ARs in determining interannual variability in NDVI.

In the dryland ecoregions, the correlation patterns were also influenced by topographic barriers and the entry into the interior west of ARs and other parts of the associated synoptic weather conditions. For example, lower-latitude ARs entering the region south of the Sierra Nevada and passing over the Mojave Desert encounter fewer mountain barriers until they reach the ranges at the transition from the Mojave to Central Basin and Range (Figure 1). Here NDVI correlations with AR precipitation tend to be higher, as the vapor transported into the area from the landfalling ARs encounters this topographic transition with resulting orographic precipitation. Farther north, correlations between AR precipitation and NDVI tend to be low across the Central Basin and Range but increase in areas as distant as northern Nevada and southwestern Wyoming (Figure 5). This pattern may, in part, reflect the fact that most mountain ranges in the Central Basin and Range are oriented parallel to the north-northeastward water vapor transports entering the region from the lower-latitude AR landfalls, whereas mountain ranges farther north are oriented in more east-west directions and might again impose renewed orographic uplift there. However, precipitation along the northern edge of the study area also occurs during these southern AR landfalls in some cases when the low-pressure center that the AR is ultimately flowing toward enters into the interior at or near the northern edge of the study area with its own compliment of storm dynamics and precipitation. Fast moving ARs also can appear in the chronology used here as making landfall at multiple latitude bands within the same day, so that some precipitation along the northern parts of the study area on a day with a southern landfall can even derive from more northern landfalls earlier the same day.

4.2. Winter AR Influences on Area Burned by Wildfire

Correlations between AR precipitation and area burned by wildfire in the Sierra Nevada and Cascades ecoregions of California are generally weak. In these ecoregions, where fuel flammability—rather than availability—is known to affect fire patterns, winter precipitation has been identified as an important predictor of fire activity but only in combination with temperature and drought conditions [e.g., *Littell et al*., 2009]. Thus, despite the strong influences of ARs on snowpack and water supplies in the Sierra Nevada of California [*Guan et al*., 2010; *Dettinger et al*., 2011], the present results suggest that winter ARs, alone, are not sufficient to determine wildfire patterns in the montane ecoregions. Correlations between AR precipitation and area burned by wildfire were generally lower for the Sonoran Desert ecoregions than for the Northern, Central, and Mojave Basin and Range ecoregions despite this region having some of the strongest AR-NDVI correlations. The Sonoran Desert ecoregions had fewer fires during the study period [*MTBS*, 2016a] as it is generally more arid, and thus fuel limited, relative to ecoregions to the north, which may have influenced the

correlations. Second, summer monsoonal precipitation significantly affects fuel moistures in the Sonoran region and is not included in our analysis.

Notably, the areas where ARs had the greatest influences on vegetation and fire patterns, such as in the Northern, Central, and Mojave Basin and Range ecoregions (and to a lesser degree in the Sonoran Desert), have experienced rapid expansions of nonnative annual plants that have occurred over the past several decades, and have continued to spread due to their ability to germinate in early winter, and thus more readily take advantage of available water resources. These species are largely responsible for the modern spread of wildfire in these regions [*Whisenant*, 1990; *Brooks*, 1999]. Our results suggest that ARs may play a significant role in the invasive grass-fire cycle in this region. This connection may have significant implications for wildfire under climate change, although it is unclear just how changing AR frequencies or intensities may interact with the cycle.

5. Conclusions

Our results are the first to indicate that low-latitude AR landfalls in the southwestern USA can influence precipitation amounts, and thus vegetation and wildfire, in distant dryland and desert ecoregions—as much as 1300 km to the north of their initial impacts along the Pacific coast. These lower-latitude ARs are increasingly being recognized for their influence on hydroclimatic variability [*Rutz and Steenburgh*, 2012; *Rutz et al*., 2014] and their roles in extreme precipitation and flooding [e.g., *Neiman et al*., 2013; *Rivera et al*., 2014] in the interior Southwest. The extent to which these events drive ecological patterns and processes in southwestern ecosystems is only now being recognized and quantified.

This study suggests strong links between interannual variations of low-latitude ARs, vegetation and fuels production, and fire in the Mojave, Central, and Northern Basin and Range ecoregions. Specifically, ARs correlate well with variability of winter precipitation, which in turn correlates with variability of annual vegetation and wildfire, in these ecoregions. These linkages may offer opportunities to enhance range management and fire prediction and forecasting in this region, especially if reliable long-lead forecastability of AR statistics can be developed. As knowledge and prediction of AR arrivals increase, seasonal or longer-term AR forecasts could, for example, help to guide timing vegetation rehabilitation treatments to enhance probabilities of success or could inform adjustments to annual operating plans to reduce livestock grazing pressure on arid rangelands in anticipation of lower AR frequencies. Still, the results presented here are based on simple correlations over a limited study period. Although we confirmed early in our study that annual AR precipitation does not covary with non-AR precipitation in a given year, additional study is needed to determine whether other potential covarying drivers are playing a significant role and to confirm causation of the AR-vegetation-wildfire linkages. As a next step, we are organizing to develop and use mechanistic models of precipitation-soils-fuels interactions to explore causal links underlying the correlations reported here.

Our results, and their potential application to natural resource management in the southwestern U.S., underscore several important implications and avenues for research. For example, the most significant influences of ARs on vegetation productivity and fire patterns occurred in association with relatively infrequent ARs making landfall within a fairly narrow band of latitudes between 25–35°, landfall locations that in many cases are seemingly far removed and irrelevant to the landscapes and vegetation in question (e.g., the areas near the Nevada/Idaho border in the Northern Basin and Range ecoregion). These lower-latitude ARs have been relatively less well studied, given that most previous research on ARs has focused on floods and water supplies in coastal ranges and the Sierra Nevada, north of about 35°N [e.g., *Neiman et al*., 2008; *Dettinger et al*., 2011; *Guan et al*., 2012; *Hagos et al*., 2016]. Our study further highlights the sensitivity of dryland ecosystems in the interior Southwest to interannual variability of landfalling ARs, so that changes in AR-landfall statistics, which have been projected under climate change [*Gao et al*., 2015], may have significant impact on the interior Southwest in coming decades. These changes could be particularly consequential where AR variability interacts with the invasive-driven annual-fire cycle that has emerged across the study region. New research is needed to deepen understanding of the historical (and potentially changing) relations between AR climatologies and vegetation/wildfire variability found here. More focus on AR landfalls south of 35°N is probably needed for application to land management in the interior Southwest.

Acknowledgments

This material is based upon the work supported by the U.S. Geological Survey under grant agreement G14AP00101 from the Southwest Climate Science Center, which is managed by the USGS National Climate Change and Wildlife Science Center. We thank Jonathan Rutz for use of his atmospheric river chronology and two anonymous reviewers for their thoughtful comments that greatly improved this paper. Data and results from this study are available at https://www.sciencebase.gov/catalog/item/544e9541e4b024090689132b.

References

Abatzoglou, J. T. (2013), Development of gridded surface meteorological data for ecological applications and modelling, *Int. J. Climatol.*, *33*(1), 121–131, doi:10.1002/joc.3413.

Abatzoglou, J. T., and C. A. Kolden (2013), Relationships between climate and macroscale area burned in the western United States, *Int. J. Wildl. Fire*, *22*, 1003–1020.

Alexander, M. A., J. D. Scott, D. Swales, M. Hughes, K. Mahoney, and C. A. Smith (2015), Moisture pathways into the US intermountain west associated with heavy winter precipitation events, *J. Hydrometeorol.*, *16*, 1184–1206, doi:10.1175/JHM-D-14-0139.1.

Brands, S., J. M. Gutiérrez, and D. San-Martín (2016), Twentieth-century atmospheric river activity along the west coasts of Europe and North America: Algorithm formulation, reanalysis uncertainty and links to atmospheric circulation patterns, *Clim. Dyn.*, doi:10.1007/s00382-016-3095-6.

Brooks, M. (1999), Alien annual grasses and fire in the Mojave Desert, *Madroño*, *46*(1), 13–19.

Crimmins, M., and A. C. Comrie (2004), Interactions between antecedent climate and wildfire variability across south-eastern Arizona, *Int. J. Wil*, *13*, 455–466.

Daly, C., M. Halbleib, J. I. Smith, W. P. Gibson, M. K. Doggett, G. H. Taylor, J. Curtis, and P. A. Pasteris (2008), Physiographically-sensitive mapping of temperature and precipitation across the conterminous United States, *Int. J. Climatol.*, *28*, 2031–2064.

Dawdy, D. R., and N. C. Matalas (1964), Statistical and probability analysis of hydrologic data, part III: Analysis of variance, covariance and time series, in *Handbook of Applied Hydrology, a Compendium of Water-Resources Technology*, edited by Ven Te Chow, pp. 8.68–8.90, McGraw-Hill Book Co., New York.

Dettinger, M. (2011), Climate change, atmospheric rivers, and floods in california – A multimodel analysis of storm frequency and magnitude changes, *J. Am. Water Resour. Assoc.*, *47*(3), 514–523, doi:10.1111/j.1752-1688.2011.00546.x.

Dettinger, M. D. (2013), Atmospheric rivers as drought busters on the U.S. West Coast, *J. Hydrometeorol.*, *14*(6), 1721–1732, doi:10.1175/JHM-D-13-02.1.

Dettinger, M. D., and L. Ingram (2013), The coming megafloods, *Sci. Am.*, *308*, 64–71.

Dettinger, M. D., F. M. Ralph, T. Das, P. J. Neiman, and D. R. Cayan (2011), Atmospheric rivers, floods and the water resources of California, *Water*, *3*(4), 445–478, doi:10.3390/w3020445.

Eidenshink, J. C. (2006), A 16-year time series of 1 km AVHRR satellite data of the conterminous United States and Alaska, *Photogramm. Eng. Rem. Sens.*, *72*, 1027–1035.

Environmental Protection Agency (2013), Level III and IV ecoregions of the continental United States. [Available at http://archive.epa.gov/wed/ecoregions/web/html/level_iii_iv-2.html#Level IV, accessed 2016-01-11.]

Florsheim, J. L., and M. D. Dettinger (2015), Promoting atmospheric-river and snowmelt fueled biogeomorphic processes by restoring river-floodplain connectivity in California's central valley, in *Geomorphology and Management of Embanked Floodplains—North American and European Fluvial Systems in an Era of Global Environmental Change*, edited by P. Hudson and H. Middelkoop, pp. 1–21, Springer, Verlag.

Gao, Y., J. Lu, L. R. Leung, Q. Yang, S. Hagos, and Y. Qian (2015), Dynamical and thermodynamical modulations on future changes of landfalling atmospheric rivers over western North America, *Geophys. Res. Lett.*, *42*, 7179–7186, doi:10.1002/2015GL065435.

Guan, B., N. P. Molotch, D. E. Waliser, E. J. Fetzer, and P. J. Neiman (2010), Extreme snowfall events linked to atmospheric rivers and surface air temperature via satellite measurements, *Geophys. Res. Lett.*, *37*, L20401, doi:10.1029/2010GL044696.

Guan, B., D. E. Waliser, N. P. Molotch, E. J. Fetzer, and P. J. Neiman (2012), Does the Madden–Julian oscillation influence wintertime atmospheric rivers and snowpack in the Sierra Nevada?, *Mon. Weather Rev.*, *140*(2), 325–342, doi:10.1175/MWR-D-11-00087.1.

Hagos, S. M., L. R. Leung, J. Yoon, J. Lu, and Y. Gao (2016), A projection of changes in landfalling atmospheric river frequency and extreme precipitation over western North America from the Large Ensemble CESM simulations, *Geophys. Res. Lett.*, *43*, 1357–1363, doi:10.1002/2015GL067392.

Hughes, M., K. M. Mahoney, P. J. Neiman, B. J. Moore, M. Alexander, and F. M. Ralph (2014), The landfall and inland penetration of a flood-producing atmospheric river in Arizona. Part II: Sensitivity of modeled precipitation to terrain height and atmospheric river orientation, *J. Hydrometeorol.*, *15*(5), 1954–1974, doi:10.1175/JHM-D-13-0176.1.

Ji, L., and A. J. Peters (2007), Performance evaluation of spectral vegetation indices using a statistical sensitivity function, *Remote Sens. Environ.*, *106*(1), 59–65, doi:10.1016/j.rse.2006.07.010.

Jones, C., and L. M. V. Carvalho (2014), Sensitivity to Madden–Julian oscillation variations on heavy precipitation over the contiguous United States, *Atmos. Res.*, *147–148*, 10–26, doi:10.1016/j.atmosres.2014.05.002.

Kalnay, E., M. Kanamitsu, R. Kistler, W. Collins, and D. Deaven (1996), The NCEP/NCAR 40-year reanalysis project, *Bull. Am. Meteorol. Soc.*, *77*, 437–471.

Kitzberger, T., P. M. Brown, E. K. Heyerdahl, T. W. Swetnam, and T. T. Veblen (2007), Contingent Pacific-Atlantic Ocean influence on multicentury wildfire synchrony over western North America, *Proc. Natl. Acad. Sci. U. S. A.*, *104*(2), 543–548, doi:10.1073/pnas.0606078104.

Knapp, A. K., and M. D. Smith (2001), Variation among biomes in temporal dynamics of aboveground primary production, *Science*, *291*(5503), 481–484, doi:10.1126/science.291.5503.481.

Lavers, D. A., G. Villarini, R. P. Allan, E. F. Wood, and A. J. Wade (2012), The detection of atmospheric rivers in atmospheric reanalyses and their links to British winter floods and the large-scale climatic circulation, *J. Geophys. Res.*, *117*, D20106, doi:10.1029/2012JD018027.

Littell, J., D. McKenzie, D. L. Peterson, and A. Westerling (2009), Climate and wildfire area burned in western U. S. ecoprovinces, 1916–2003, *Ecol. Appl.*, *19*(4), 1003–1021.

Liu, X., X. Ren, and X.-Q. Yang (2015), Decadal changes in multi-scale water vapor transport and atmospheric river associated with the pacific decadal oscillation and the north pacific gyre oscillation, *J. Hydrometeorol.*, 273–285, doi:10.1175/JHM-D-14-0195.1.

Monitoring Trends in Burn Severity (2016a), National MTBS burned area boundaries dataset. [Available at http://www.mtbs.gov/national-regional/burnedarea.html, accessed 2016-01-11.]

Monitoring Trends in Burn Severity (2016b) National MTBS burn severity mosaics. [Available at http://www.mtbs.gov/nationalregional/download.html, accessed 2016-01-11.]

Mundhenk, B. D., E. A. Barnes, E. D. Maloney, and K. M. Nardi (2016), Modulation of atmospheric rivers near Alaska and the U.S. West Coast by northeast Pacific height anomalies, *J. Geophys. Res. Atmos.*, *121*, 12,712–751,765, doi:10.1002/2016JD025350.

Neiman, P. J., F. M. Ralph, G. A. Wick, J. D. Lundquist, and M. D. Dettinger (2008), Meteorological characteristics and overland precipitation impacts of atmospheric rivers affecting the West Coast of North America based on eight years of SSM/I satellite observations, *J. Hydrometeorol.*, *9*(1), 22–47, doi:10.1175/2007JHM855.1.

Neiman, P. J., F. M. Ralph, B. J. Moore, M. Hughes, K. M. Mahoney, J. M. Cordeira, and M. D. Dettinger (2013), The landfall and inland penetration of a flood-producing atmospheric river in Arizona. Part I: Observed synoptic-scale, orographic, and hydrometeorological characteristics, *J. Hydrometeorol.*, *14*(2), 460–484, doi:10.1175/JHM-D-12-0101.1.

Notaro, M., Z. Liu, R. G. Gallimore, J. W. Williams, D. S. Gutzler, and S. Collins (2010), Complex seasonal cycle of ecohydrology in the Southwest United States, *J. Geophys. Res.*, *115*, G04034, doi:10.1029/2010JG001382.

Owen, G., J. McCleod, C. A. Kolden, D. Ferguson, and T. J. Brown (2012), Wildfire management and forecasting fire potential: The roles of climate information and social networks in the Southwest US, *Weather. Clim. Soc.*, *4*, 90–102.

Payne, A. E., and G. Magnusdottir (2015), An evaluation of atmospheric rivers over the North Pacific in CMIP5 and their response to warming under RCP 8.5, *J. Geophys. Res. Atmos.*, *120*, 11,111–173,190, doi:10.1002/2015JD023586.

Pettorelli, N., J. O. Vik, A. Mysterud, J. M. Gaillard, C. J. Tucker, and N. C. Stenseth (2005), Using the satellite-derived NDVI to assess ecological responses to environmental change, *Trends Ecol. Evol.*, *20*(9), 503–510, doi:10.1016/j.tree.2005.05.011.

Ralph, F. M., P. J. Neiman, G. A. Wick, S. I. Gutman, M. D. Dettinger, D. R. Cayan, and A. B. White (2006), Flooding on California's Russian River: Role of atmospheric rivers, *Geophys. Res. Lett.*, *33*, L13801, doi:10.1029/2006GL026689.

Ralph, F. M., T. Coleman, P. J. Neiman, R. J. Zamora, and M. D. Dettinger (2013), Observed impacts of duration and seasonality of atmospheric-river landfalls on soil moisture and runoff in coastal northern California, *J. Hydrometeorol.*, *14*(2), 443–459, doi:10.1175/JHM-D-12-076.1.

Ralph, F. M., et al. (2016), CalWater field studies designed to quantify the roles of atmospheric rivers and aerosols in modulating U.S. West Coast precipitation in a changing climate, *Bull. Am. Meteorol. Soc.*, *97*(7), 1209–1228, doi:10.1175/BAMS-D-14-00043.1.

Ralph, M. F., and M. D. Dettinger (2012), Historical and national perspectives on extreme West Coast precipitation associated with atmospheric rivers during December 2010, *Bull. Am. Meteorol. Soc.*, *93*, 783–790, doi:10.1175/BAMS-D-11-00188.1.

Ralph, M. F., P. J. Neiman, D. E. Kingsmill, P. O. G. Persson, A. B. White, E. T. Strem, E. D. Andrews, and R. C. Antweiler (2003), The impact of a prominent rain shadow on flooding in California's Santa Cruz Mountains: A CALJET case study and sensitivity to the ENSO cycle, *J. Hydrometeorol.*, *4*, 1243–1264.

Reed, B. C., J. F. Brown, D. VanderZee, T. R. Loveland, J. W. Merchant, and D. O. Ohlen (1994), Measuring phenological variability from satellite imagery, *J. Veg. Sci.*, *5*(5), 703–714, doi:10.2307/3235884.

Rivera, E. R., F. Dominguez, and C. L. Castro (2014), Atmospheric rivers and cool season extreme precipitation events in the Verde River basin of Arizona, *J. Hydrometeorol.*, *15*(2), 813–829, doi:10.1175/JHM-D-12-0189.1.

Rutz, J. J., and W. J. Steenburgh (2012), Quantifying the role of atmospheric rivers in the interior western United States, *Atmos. Sci. Lett.*, *13*(4), 257–261, doi:10.1002/asl.392.

Rutz, J. J., W. J. Steenburgh, and F. M. Ralph (2014), Climatological characteristics of atmospheric rivers and their inland penetration over the western United States, *Mon. Weather Rev.*, *142*(2), 905–921, doi:10.1175/MWR-D-13-00168.1.

Swetnam, T. W., and J. L. Betancourt (1997), Mesoscale ecological responses to climatic variability in the American Southwest, *J. Clim.*, *11*, 3128–1347, doi:10.1007/978-90-481-8736-2_32.

Swets, D. L., Reed, B. C., Rowland, J. R., and S. E. Marko (1999), A weighted least-squares approach to temporal smoothing of NDVI, in *Proceedings of the 1999 ASPRS Annual Conference, from Image to Information*, Portland, Oregon, May 17-21, 1999, Am. Soc. for Photogrammetry and Remote Sensing. [Available at https://phenology.cr.usgs.gov/pubs/ASPRS%20Swets%20et%20al%20Smoothing.pdf.]

Warner, M. D., C. F. Mass, and E. P. Salathé (2014), Changes in winter atmospheric rivers along the North American west coast in CMIP5 climate models, *J. Hydrometeorol.*, *16*, 118–128, doi:10.1175/JHM-D-14-0080.1.

Westerling, A. L., A. Gershunov, T. J. Brown, D. R. Cayan, and M. D. Dettinger (2003), Climate and wildfire in the western United States, *Bull. Am. Meteorol. Soc.*, *84*(5), 595–604, doi:10.1175/BAMS-84-5-595.

Whisenant, S. G. (1990), Changing fire frequencies on Idaho's Snake River Plains: Ecological and management implications, in *Symposium on Cheatgrass Invasion, Shrub Die-Off and other aspects of Shrub Biology and Management, USDA Forest Service General Tech. Rep. INT-276*, edited by E. D. McArthur et al., pp. 4–10, Las Vegas, Nev.

Wick, G. A., P. J. Neiman, F. M. Ralph, and T. M. Hamill (2013), Evaluation of forecasts of the water vapor signature of atmospheric rivers in operational numerical weather prediction models, *Weather Forecast.*, *28*(6), 1337–1352, doi:10.1175/WAF-D-13-00025.1.